Gears

Complements of Machine Elements

Carlos Fernandes

2024

Mestrado em Engenharia Mecânica

Recommended bibliography

- Henriot, Georges; Engrenages. ISBN: 2-10-003903-2
- Fernandes, C. M. C. G., Marques, P. M. T., Martins, R. C., Seabra, J. H. O. (2015). Gearbox power loss. Part II: Friction losses in gears. Tribology International, 88(0)
- MAAG Gear Company, Ltd.; MAAG gear book
- Branco, C. M., Ferreira, J. M., Costa, J. D., Ribeiro, A. S.; Projecto de Órgãos de Máquinas, Fundação Calouste Gulbenkian

Gear Standards

- NF E 23-001: Vocabulaire des Engrenages: Definitions Géométriques
- NF E 23-002: Vocabulaire des Engrenages: Definitions Géométriques Engrenages à vis
- NF E 23-011: Engrenages: Crémaillére de Référence et Modules des Rous Cylindriques à Developpante de Mécnique Générale et de Grosse Méchanique
- NF E 23-012: Engrenages Cylindriques: Indications à Fournir au Fabricant d'Engrenages
- NF E 23-013: Engrenages: Déport de Dentures des Roues Cylindriques pour Engrenages Réducteurs

Gear Standards

- DIN 780: Series of modules for gears
- DIN 867: Basic rack of Cylindrical Gears with Involute Teeth for General and Heavy Engineering
- DIN 868: General Definitions and Specification Factors for Gears, Gear Pairs and Gear Trains
- DIN 3960: Concepts and parameters associated with cylindrical gears and cylindrical gear pairs with involute teeth
- DIN 3972: Reference Profiles of Gear-cutting Tools for Involute Tooth Systems according to DIN 867
- DIN 3975: Terms and Definitions for Cylindrical Worm Gears with Saft Angle 90°

Gear Standards

- DIN 3978: Helix Angles for Cylindrical Gear Teeth
- DIN 3979: Tooth Damage on Gear Trains: Designation, Characteristics, Causes
- DIN 3998: Denominations on gears and gear pairs
- NP EN ISO 2203: Desenhos técnicos - Representação convencional de engrenagens
- ISO 6336: Calculation of load capacity of spur and helical gears

Hyperlink

Lecture 1

Summary

Introduction

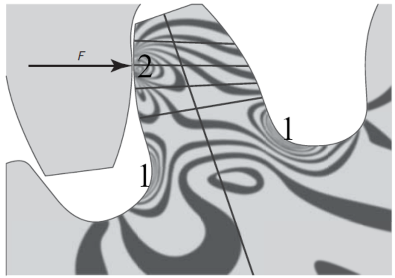

Figure 1: Photoelastic pattern of stresses in a spur gear tooth [1].

The experimental stress analysis presented in Figure 1 shows that highest stresses exist where the lines are bunched closest together.

This occurs at two locations: (1) the fillet at the base of the tooth and (2) the point of contact with the mating gear, where force *F* is acting.

There are two main components limiting gear load carrying capacity:

1. **tooth bending and fatigue**
2. **contact pressure.**

Forces on gearing

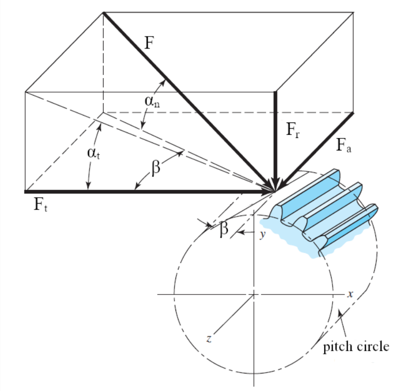

Figure 2: Forces in a right helical gear [2].

Tangential:

$$F_t = \frac{M_t}{r} = \frac{P}{v}$$

Normal:

$$F_n = \frac{F_t}{\cos \alpha_t}$$

Radial:

$$F_r = F_t \cdot \tan \alpha_t$$

Axial:

$$F_a = F_t \cdot \tan \beta$$

Root bending

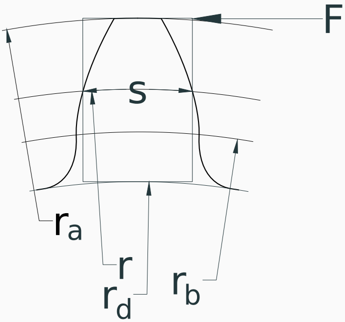

Figure 3: Simplified model for the tooth root bending.

Considering the face width b, the tooth section can be approximated as $s \times b$ and height h:

$$h = r_a - r_d = 2.25 \cdot m$$

The tangential force is calculated by:

$$F = F_t = \frac{M_t}{r}$$

The bending moment on the tooth root with radius r_d is:

$$M_f = F_t \cdot h$$

Root bending

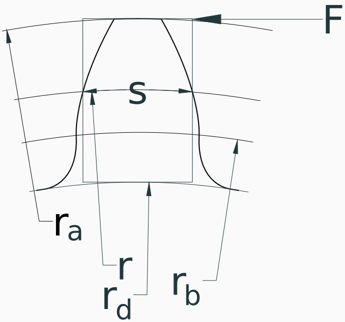

Figure 3: Simplified model for the tooth root bending.

The maximum stress on the tooth root (traction on the right, compression on the left) is:

$$\sigma = \frac{M_f \cdot y_{max}}{I}$$

With:

$$y_{max} = \frac{s}{2}$$

$$I = \frac{b \cdot s^3}{12}$$

Root bending

For a gear without profile shift, $x = 0$, the tooth thickness on the pitch radius is $s = \frac{\pi \cdot m}{2}$

$$\sigma = \frac{F_t \cdot h \cdot \frac{s}{2}}{\frac{b \cdot s^3}{12}} = \frac{6 \cdot F_t \cdot h}{b \cdot s^2} = \frac{6 \cdot F_t \cdot 2.25 \cdot m}{b \cdot \left(\frac{\pi \cdot m}{2}\right)^2} = \frac{54 \cdot F_t}{\pi^2 \cdot b \cdot m} = \frac{5.471 \cdot F_t}{b \cdot m} \leq \sigma_{adm}$$

Expressing the face width b as a function of the module $b = k \cdot m$, we can write the previous equation to select the module m:

$$\frac{5.471 \cdot F_t}{k \cdot m^2} \leq \sigma_{adm} \Leftrightarrow m \geq \sqrt{\frac{5.471 \cdot F_t}{k \cdot \sigma_{adm}}}$$

This module is very coarse and is not used in practice.

Lewis formula

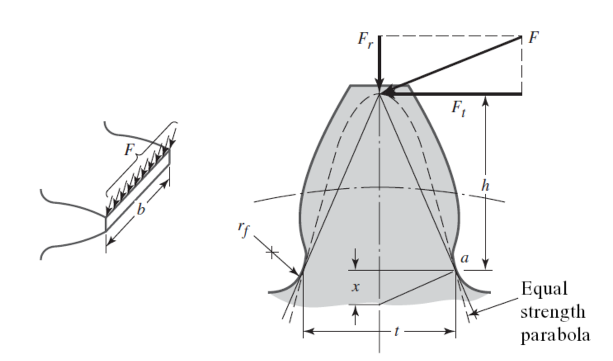

Figure 4: Lewis model to define critical section for root bending [1].

- The full load is applied to the tip of a single tooth;
- The radial component F_r is negligible;
- The load is distributed uniformly across the full face width;
- Forces which are due to tooth sliding friction are negligible;
- Stress concentration in the tooth fillet is negligible.

Lewis formula

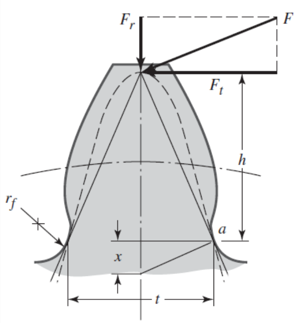

Figure 5: Lewis model to define critical section for root bending [1].

$$\sigma = \frac{F_t \cdot h \cdot \frac{t}{2}}{\frac{b \cdot t^3}{12}} = \frac{6 \cdot F_t \cdot h}{b \cdot t^2}$$

Similar triangles:

$$\frac{t/2}{x} = \frac{h}{t/2} \Leftrightarrow \frac{t^2}{h} = 4 \cdot x$$

$$\boxed{\sigma = \frac{F_t}{\pi \cdot b \cdot m \cdot y}}$$

$$y = \frac{4 \cdot x}{6 \cdot \pi \cdot m}$$

For a pressure angles of $\alpha = 20°$ [3, 4]:

$$y = 0.154 - 0.912/z$$

Lewis formula

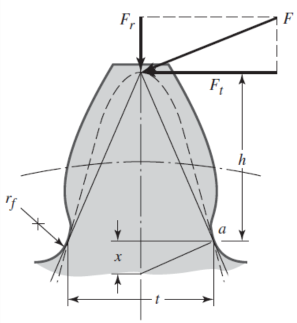

Figure 5: Lewis model to define critical section for root bending [1].

$$\sigma = \frac{F_t}{\pi \cdot b \cdot m \cdot y}$$

The tangential force written as function of the transmitted torque: $F_t = \frac{M_t}{r}$

The face width as a function of gear module: $b = k \cdot m$:

$$\sigma = \frac{\frac{M_t}{\frac{z \cdot m}{2}}}{\pi \cdot k \cdot m \cdot m \cdot y} \leq \sigma_{adm}$$

The module is then estimated as:

$$\boxed{m \geq \sqrt[3]{\frac{2 \cdot M_t}{\pi \cdot k \cdot z \cdot y \cdot \sigma_{adm}}}}$$

Lewis formula

$$\sigma = \frac{F_t}{\pi \cdot b \cdot m \cdot y}$$

A typical way to write the Lewis formula is:

$$\sigma = \frac{F_t}{\pi \cdot b \cdot m \cdot y} = \frac{F_t}{bm} Y$$

Where $Y_L = \frac{1}{\pi y}$

The tangential force written as function of the transmitted torque: $F_t = \frac{M_t}{r}$

The face width as a function of gear module: $b = k \cdot m$:

$$\sigma = \frac{\frac{M_t}{\frac{z \cdot m}{2}}}{\pi \cdot k \cdot m \cdot m \cdot y} \leq \sigma_{adm}$$

The module is then estimated as:

$$\boxed{m \geq \sqrt[3]{\frac{2 \cdot M_t}{\pi \cdot k \cdot z \cdot y \cdot \sigma_{adm}}}}$$

Lewis formula

Table 18-1. Lewis Form Factors y

Number of teeth	External gears: 14½-deg composite system $a = 1/P$ *	External gears: 20-deg full-depth system $a = 1/P$	External gears: 20-deg stub system $a = 0.80/P$	Internal gears, 20-deg full-depth system: Pinion $a = 1/P$	Internal gears, 20-deg full-depth system: Internal gear $a = 1/P$
10	0.055	0.064	0.088	0.103	
11	0.062	0.072	0.093	0.104	
12	0.067	0.078	0.099	0.104	
13	0.071	0.083	0.103	0.104	
14	0.075	0.088	0.108	0.105	
15	0.078	0.092	0.111	0.105	
16	0.081	0.094	0.115	0.106	
17	0.084	0.096	0.117	0.109	
18	0.086	0.098	0.120	0.111	
19	0.088	0.100	0.123	0.114	
20	0.090	0.102	0.125	0.116	
21	0.092	0.104	0.127	0.118	
22	0.093	0.105	0.129	0.119	
24	0.095	0.107	0.132	0.122	
26	0.098	0.110	0.135	0.125	
28	0.100	0.112	0.137	0.127	0.220
30	0.101	0.114	0.139	0.129	0.216
34	0.104	0.118	0.142	0.132	0.210
38	0.106	0.122	0.145	0.135	0.205
43	0.108	0.126	0.147	0.137	0.200
50	0.110	0.130	0.151	0.139	0.195
60	0.113	0.134	0.154	0.142	0.190
75	0.115	0.138	0.158	0.144	0.185
100	0.117	0.142	0.161	0.147	0.180
150	0.119	0.146	0.165	0.149	0.175
300	0.122	0.150	0.170	0.152	0.170
Rack	0.124	0.154	0.175		

* a = addendum; P = diametral pitch.

Figure 6: Lewis form factor according to [5].

$$Y_L = \frac{1}{\pi \cdot y}$$

The values of y are typically listed in Tables.

An approximate equation was proposed by Wallace [4]. For pressure angle $\alpha = 20°$:

$$y = 0.154 - 0.912/z$$

For $\alpha = 14.5°$

$$y = 0.124 - 0.684/z$$

Lewis formula

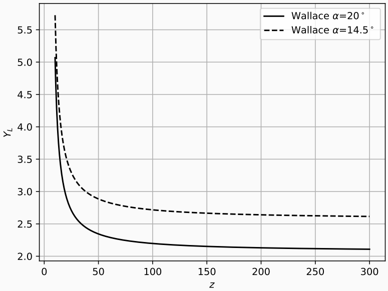

Figure 7: Lewis form factor.

A conservative way is to use the biggest Lewis form factor:

$$\boxed{m \geq \sqrt[3]{\frac{10 \cdot M_t}{z \cdot k \cdot \sigma_{adm}}}}$$

A similar equation can be found in German design guideline VDI 2736 Part 2 for plastic gears [6]:

$$\boxed{m \geq \sqrt[3]{\frac{6 \cdot M_t}{z \cdot k \cdot \sigma_{adm}}}}$$

From $Y_L = \frac{1}{\pi y}$:

$$\boxed{m \geq \sqrt[3]{\frac{2 \cdot M_t}{\pi \cdot k \cdot z \cdot y \cdot \sigma_{adm}}}}$$

ISO critical section

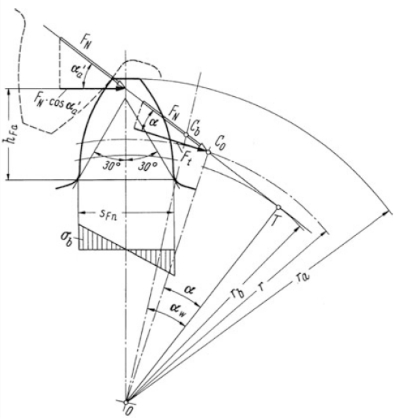

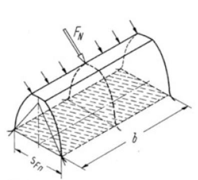

Figure 8: Tooth root critical section s_{Fn} according to ISO [7].

$$
\begin{aligned}
\sigma_b &= \frac{(F_t \cdot h_{Fa}) \cdot (s_{Fn}/2)}{\frac{b \cdot {s_{Fn}}^3}{12}} \\
&= \frac{\left(F_N \cdot \cos\alpha_a' \cdot h_{Fa}\right) \cdot (s_{Fn}/2)}{\frac{b \cdot {s_{Fn}}^3}{12}} \\
&= \frac{6 \cdot F_N \cdot \cos\alpha_a' \cdot h_{Fa}}{b \cdot {s_{Fn}}^2}
\end{aligned}
$$

$$
\boxed{\sigma_b = \frac{F_t}{b \cdot m} \cdot \frac{6 \cdot \left(\frac{h_{Fa}}{m}\right) \cdot \cos\alpha_a'}{\left(\frac{s_{Fn}}{m}\right)^2 \cdot \cos\alpha} = \frac{F_t}{b \cdot m} \cdot Y_F}
$$

ISO form factor

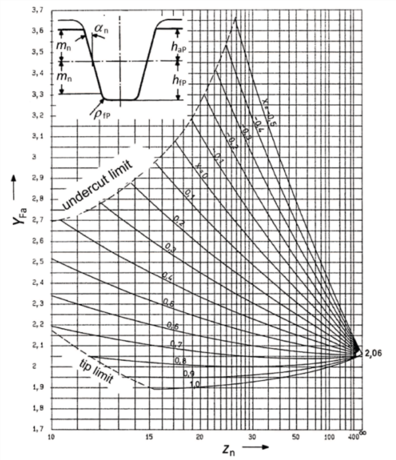

Figure 9: Form factor Y_{Fa} for $h_{fP} = 1.25 \cdot m$, $h_{aP} = m$, $\rho_{fP} = 0.25 \cdot m$ [8].

The form factor can be determined using graphical data from ISO 6336-3:1996. The number of tooth and the profile shift should be known. The graphical data should be suitable for the reference profile used.

Normal load along the path of contact

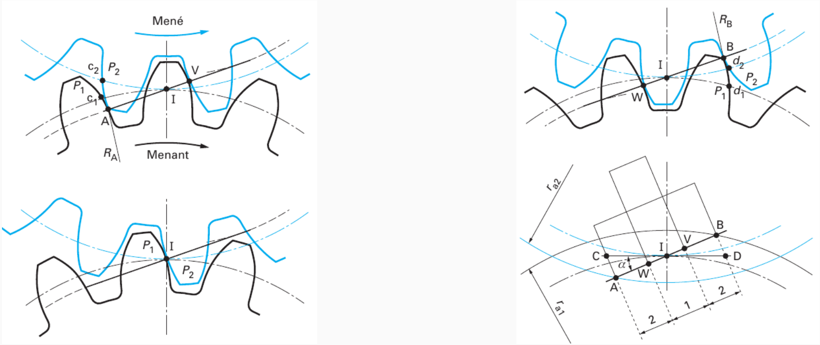

Figure 10: Load sharing along path of contact [9].

The normal force changes along the path of contact. Up to now, the equations to calculate the maximum stress considered just one tooth is carrying all the load.

Normal load along the path of contact

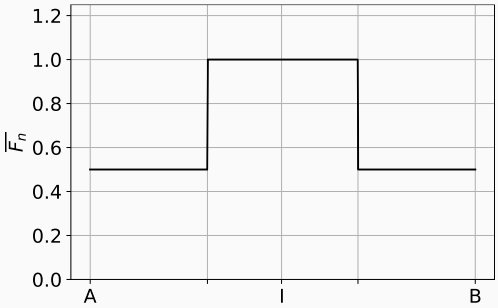

Figure 11: Load sharing function disregarding elastic effects.

$$\boxed{\sigma_b = \frac{F_t}{b \cdot m} \cdot Y_F \cdot Y_\epsilon}$$

with $Y_\epsilon = \frac{1}{\epsilon_\alpha}$. This means that the load is carried by and average number of tooth in contact equal to ϵ_α

Stress concentration at tooth root fillet

$$\sigma_{b_{lim}} = \frac{\sigma_{b,10^7}}{Y_S \cdot S_F}$$

According to Henriot [10] the average value is $Y_S = 1.8$.

The load is of repeated type, so:

$$R = \frac{F_{min}}{F_{max}} = 0$$

The amplitude load and the average load are:

$$F_a = F_m = \frac{F_{max}}{2}$$

For epicyclic gear trains

$F_{min} = -F_{max} = -F$, so:

$$R = \frac{F_{min}}{F_{max}} = -1$$

The average load is vanished on such cases:

$$F_m = \frac{F_{max} + F_{min}}{2} = 0$$

The amplitude load is:

$$F_a = \frac{F_{max} + F_{min}}{2} = F$$

Henriot states that for such case σ_b should be reduced by 25 %.

Stress concentration at tooth root fillet

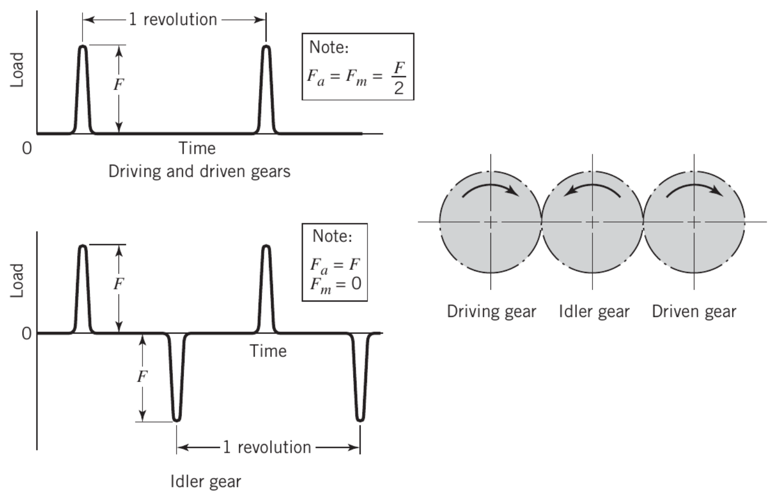

Figure 12: Load fluctuation [1].

Stress concentration at tooth root fillet

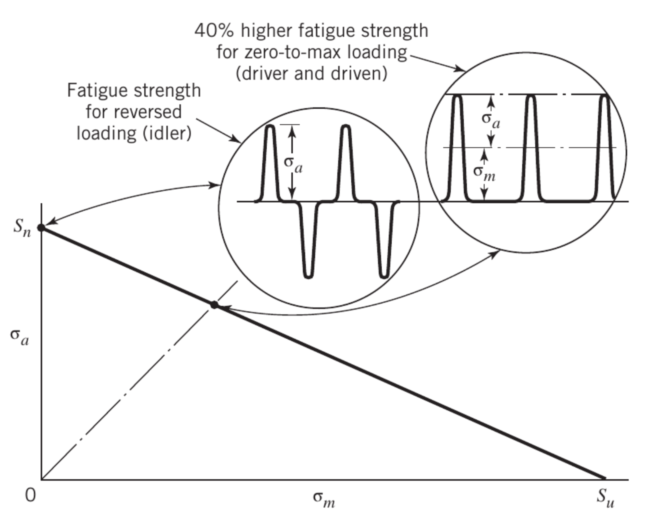

Figure 13: Stress fluctuation [1].

Stress concentration at tooth root fillet

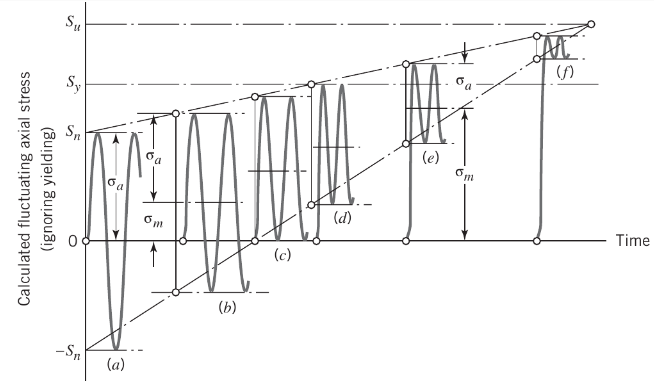

Figure 14: Various fluctuating stresses, all corresponding to equal fatigue life [1].

(a) $R = -1$ and *(c)* $R = 0$

Tooth bending fatigue testing

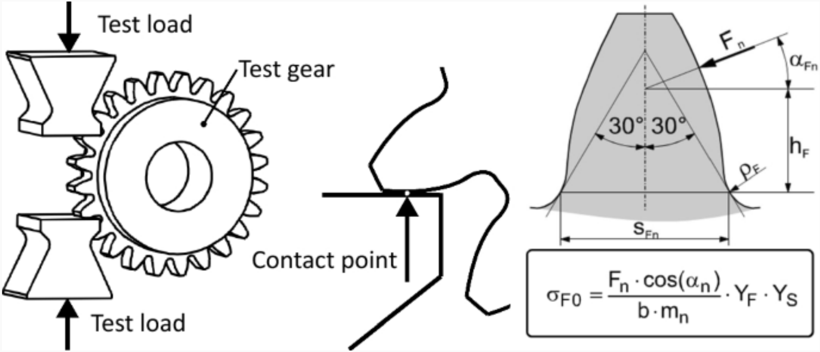

Figure 15: Tooth bending fatigue testing.

Load correction factors

There several factors that should be taken into account to refine the model presented. Henriot [10] lists:

- dynamic (speed) effect K_V
- load type K_A (for example if the system works under shock loading)
- load application duration K_{bL} (increase in the allowable stress if the duration of load application is short)
- factor depending on the ratio face width / pitch diameter $\frac{b}{d}$. For a high ratio is difficult to have theoretical conditions of gearing due to machining inaccuracies, distortions, misalignment [3]

$$\boxed{F_{t_{lim}} = \sigma_{b_{lim}} \cdot b \cdot m \cdot \frac{K_V \cdot K_A \cdot K_M \cdot K_{bL}}{Y_\epsilon \cdot Y_F \cdot Y_\beta}}$$

Lecture 2

Summary

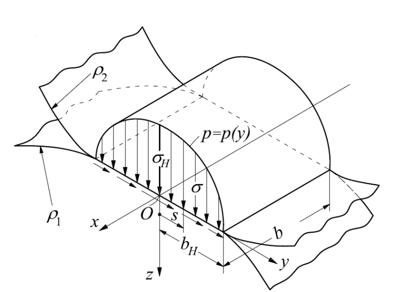

Figure 16: Hertz solution for the contact pressure between two cylinders [11].

Hertz admitted the following hypotheses for the contact of two bodies:

- Each body can be treated as an elastic half-space loaded over the small contacting area;
- The dimensions of the contact area must be small compared with the dimensions of each body and with the relative radii of curvature of the surfaces;
- The surfaces are friction-less, so only normal load is applied between them;
- The strains are small, so that Hooke's law is valid.

Contact pressure between two cylinders

$$\boxed{\sigma_H = \sqrt{\frac{F_n \cdot E^*}{\pi \cdot b \cdot \rho}}}$$

Where b is width of the shortest cylinder.

F_n is the normal force.

Equivalent Young's modulus:

$$\frac{1}{E^*} = \left(\frac{1-\nu_1^2}{E_1} + \frac{1-\nu_2^2}{E_2}\right)$$

Where E_1 and E_2 are the Young modulus of cylinder 1 and 2, respectively.

And ν_1 and ν_2 are the Poisson ratio of cylinder 1 and 2, respectively.

Relative radius:

$$\frac{1}{\rho} = \frac{1}{\rho_1} + \frac{1}{\rho_2}$$

Where ρ_1 and ρ_2 are the radius of cylinder 1 and 2, respectively.

Gear kinematics

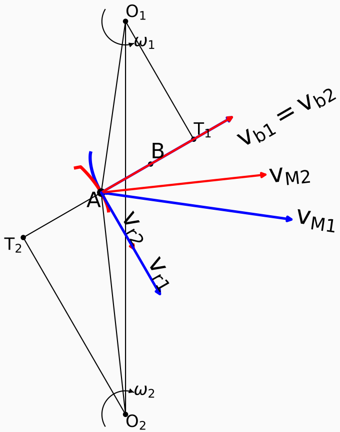

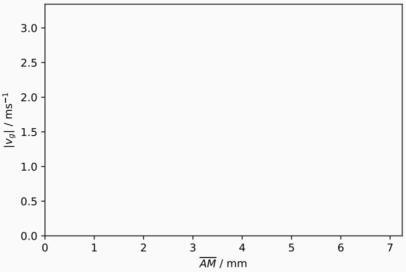

Play/Pause

Gear kinematics – rolling speeds

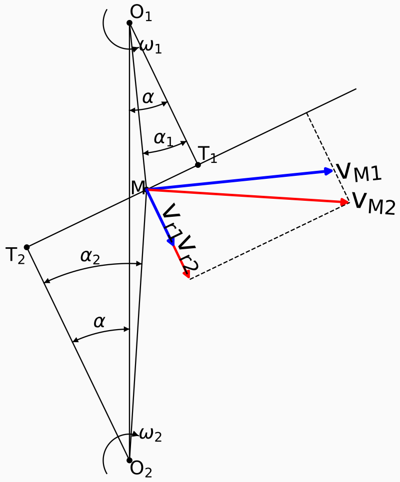

Figure 17: Rolling speeds

The rolling speeds (tangential to the contact) at contacting point M are:

$$\boxed{\begin{aligned} v_{r1} &= v_{M1} \cdot \sin\alpha_1 = (\omega_1 \cdot r_{M1}) \sin\alpha_1 \\ v_{r2} &= v_{M2} \cdot \sin\alpha_2 = (\omega_2 \cdot r_{M2}) \sin\alpha_2 \end{aligned}}$$

The difference of rolling speeds of profile 1 relative to profile 2 is the **sliding speed**.

Since there exists friction between the contacting surfaces, the sliding promotes power loss (↓ efficiency).

Conceptual cylinders

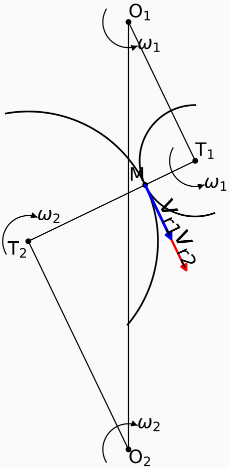

Figure 18: Conceptual cylinders

As discussed before, the rolling speeds are:

$$v_{r1} = \omega_1 \cdot r_{M1} \sin \alpha_1$$
$$v_{r2} = \omega_2 \cdot r_{M2} \sin \alpha_2$$

The tooth profiles 1 and 2 can be approximated by two circles contacting in point M with center in T_1 and T_2:

- radius $\overline{T_1 M}$ with center T_1
- radius $\overline{T_2 M}$ with center T_2

$\boxed{v_{r1} = \omega_1 \cdot \overline{T1M}}$ $\boxed{v_{r2} = \omega_2 \cdot \overline{T2M}}$

Conceptual cylinders

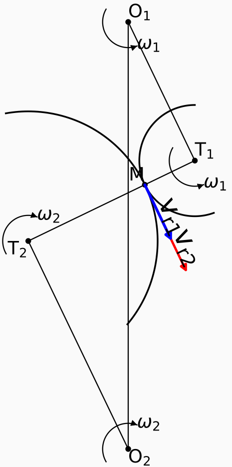

Figure 18: Conceptual cylinders

The dimensions of the conceptual cylinders at each contacting position are used to calculate the Hertz contact pressure.

The radius of the cylinders is:

$$\rho_1 = \overline{T_1 M}$$
$$\rho_2 = \overline{T_2 M}$$

Since $\overline{T_1 T_2}$ is constant, the sum of the cylinders radii is always:

$$\boxed{\rho_1 + \rho_2 = \overline{T_1 T_2}}$$

Contact pressure between mating teeth

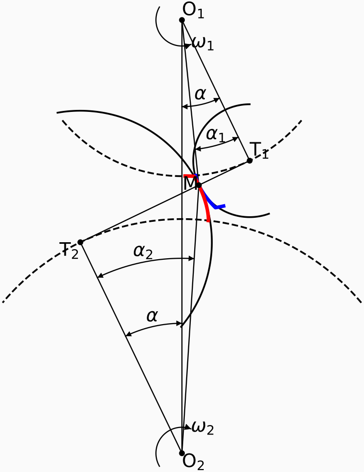

Figure 19: Conceptual cylinders at any contacting position M.

$$\boxed{\sigma_H = \sqrt{\frac{F_n \cdot E^*}{\pi \cdot b \cdot \rho}}}$$

Where b is the gear face width.

Normal force:

$$F_n = \frac{F_t}{\cos \alpha_t}$$

Equivalent Young's modulus:

$$\frac{1}{E^*} = \left(\frac{1-\nu_1^2}{E_1} + \frac{1-\nu_2^2}{E_2} \right)$$

Relative radius:

$$\frac{1}{\rho} = \frac{1}{\rho_1} + \frac{1}{\rho_2}$$

Contact pressure along the path of contact

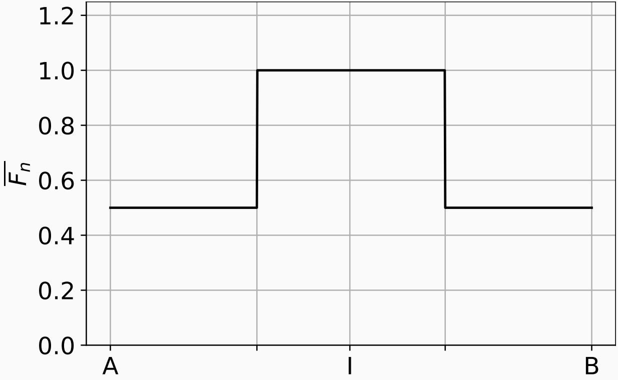

Figure 20: Load sharing function disregarding elastic effects.

As already discussed, the normal load varies along the path of contact for a spur gear as represented in the Figure 20, so the contact pressure will be affected by this.

Contact pressure along the path of contact

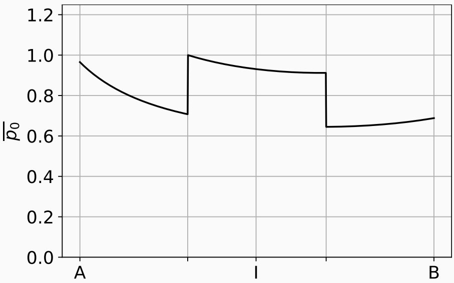

Figure 21: Normalized contact pressure along the path of contact.

The contact pressure $\sigma_H = p_0$ changes along the path of contact because:

- the relative radius ρ changes as ρ_1 and ρ_2 changes ($\overline{T_1T_2} = \rho_1 + \rho_2$);
- the normal load changes as shown in Figure 20.

A point for calculation of contact pressure is then the pitch point, since it gives a very good approximation to the maximum value of the contact pressure.

Contact pressure over the pitch circle

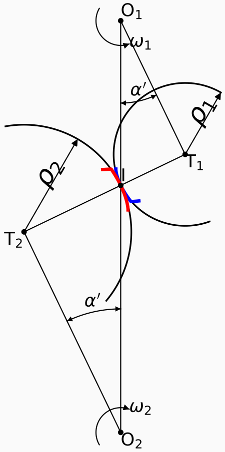

Figure 22: Conceptual cylinders over pitch circle.

$$\sigma_{H_I} = \sqrt{\frac{F_n \cdot E^*}{\pi \cdot b \cdot \rho_I}}$$

Normal force over pitch circle:

$$F_n = \frac{F_t}{\cos \alpha'_t}$$

Assuming a steel gear:

$$E_1 = E_2 = 210\,\mathrm{GPa} \text{ and } \nu_1 = \nu_2 = 0.3$$

The equivalent Young's modulus:

$$E^* = 115.385 \times 10^9 \mathrm{Pa}$$

Contact pressure over the pitch circle

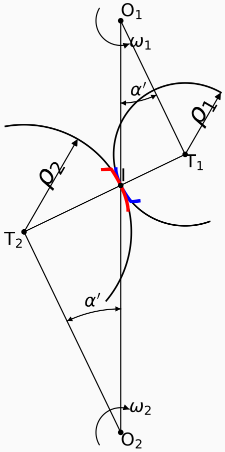

Figure 22: Conceptual cylinders over pitch circle.

Equivalent radius over pitch circle:

$$\frac{1}{\rho_I} = \left(\frac{1}{r_1' \cdot \sin \alpha'} + \frac{1}{r_2' \cdot \sin \alpha'} \right)$$

Relative radius over the pitch circle

$$\rho_I = \frac{r_1' \cdot r_2' \cdot \sin \alpha'}{r_1' + r_2'}$$

$$\sigma_{H_I} = \sqrt{\frac{F_n \cdot E^*}{\pi \cdot b \cdot \rho_I}}$$

$$\sigma_{H_I} = 192 \cdot \sqrt{\frac{F_n \cdot (r_1' + r_2')}{b \cdot r_1' \cdot r_2' \cdot \sin \alpha'}}$$

σ_{H_I} in MPa and r_1', r_2' and b in mm.

Contact pressure over the pitch circle

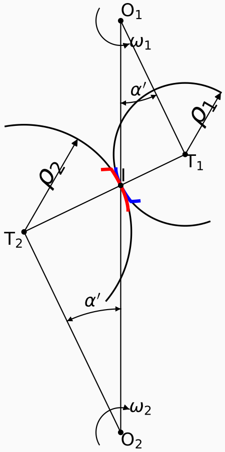

Figure 22: Conceptual cylinders over pitch circle.

$$\sigma_{H_I} = 192 \cdot \sqrt{\frac{F_n \cdot (r_1' + r_2')}{b \cdot r_1' \cdot r_2' \cdot \sin \alpha'}}$$

Making $F_{nu} = \frac{F_n}{b}$ and $a' = r_1' + r_2'$:

$$\sigma_{H_I} = 192 \cdot \sqrt{F_{nu} \frac{a'}{r_1' \cdot r_2' \cdot \sin \alpha'}}$$

Finally $u = \frac{z_2}{z_1}$ or $u = \frac{r_2'}{r_1'}$:

$$\sigma_{H_I} = 192 \cdot \sqrt{F_{nu} \cdot \frac{1}{r_1' \cdot \sin \alpha'} \cdot \frac{u+1}{u}}$$

Contact pressure over the pitch circle

But recall that:

$$F_{nu} = \frac{F_n}{b} = \frac{F_t}{b\cos\alpha} = \frac{F_t'}{b\cos\alpha'} \quad \text{and} \quad K = \frac{F_t}{b\cdot d_1}\cdot\frac{u+1}{u} = \frac{F_t'}{b\cdot d_1'}\cdot\frac{u+1}{u}$$

So, the contact stress at pitch point can be written as:

$$\sigma_{H_I} = 192\cdot\sqrt{\frac{F_t'}{b\cos\alpha'}\cdot\frac{2}{d_1'\sin\alpha'}\cdot\frac{u+1}{u}} = 192\cdot\sqrt{\frac{2}{\cos\alpha'\sin\alpha'}}\cdot\sqrt{K}$$

$$\boxed{\sigma_{H_I} = 192\cdot\sqrt{\frac{2}{\cos\alpha'\sin\alpha'}}\cdot\sqrt{\frac{F_t}{b\cdot d_1}\cdot\frac{u+1}{u}}}$$

Lecture 3

Summary

Standardization on gear load carrying capacity

The following entities has presented standards about gear load carrying capacity: AFNOR (France), AGMA (USA), BSI (UK), DIN (Germany), ISO (International)...

The main standards are:

- Alemanha
  - DIN 3990:1987 – “Calculation of load capacity of cylindrical gears”
- USA
  - AGMA 2101-D04 – “Fundamental Rating Factors and Calculation Methods for Involute Spur and Helical Gear Teeth”
- International
  - ISO 6336:1996; ISO 6336:2006; ISO 6336:2019 – “Calculation of load capacity of spur and helical gears” [12]

ISO 6336:1 Introduction

Table 1: ISO 6336:2019 [13]

Calculation of load capacity of spur and helical gears	International Standard	Technical Specification	Technical Report
Part 1: Basic principles, introduction and general influence factors	X		
Part 2: Calculation of surface durability (pitting)	X		
Part 3: Calculation of tooth bending strength	X		
Part 4: Calculation of tooth flank fracture load capacity		X	
Part 5: Strength and quality of materials	X		
Part 6: Calculation of service life under variable load	X		
Part 20: Calculation of scuffing load capacity (also applicable to bevel and hypoid gears) — Flash temperature method (replaces: ISO/TR 13989-1)		X	
Part 21: Calculation of scuffing load capacity (also applicable to bevel and hypoid gears) — Integral temperature method (replaces: ISO/TR 13989-2)		X	
Part 22: Calculation of micropitting load capacity (replaces: ISO/TR 15144-1)		X	
Part 30: Calculation examples for the application of ISO 6336 parts 1,2,3,5			X
Part 31: Calculation examples of micropitting load capacity (replaces: ISO/TR 15144-2)			X

ISO 6336-1: Scope

ISO 6336 **should be used** for the following situations [12, 13]:

- pressure angle between 15 and 25 $^\circ$;
- helix angle up to 30 $^\circ$;
- spur gears or helical gears with contact ratio $1 < \epsilon_\alpha < 2.5$;

ISO 6336 **should not be used** for the following situations [12, 13]:

- spur or helical gears with contact ratio $\epsilon_\alpha < 1$;
- interference between tooth tips and root fillets;
- teeth are pointed;
- backlash is zero.

This standard should not be used for non-metallic gears. For plastic gears, use instead VDI 2545 (1981) e VDI 2736 (2016).

ISO 6336-1: Basic Principles

Calculation methods according to ISO 6336:1996:

A - factors derived using comprehensive mathematical analysis (FEM for example) and experimental testing (seldom used due to costs);

B - factors are derived with sufficient accuracy for most applications using a rigorous geometric model;

C - factors derived using simplified approximations. On each occasion an assessment should be made as to whether or not these assumptions apply to the existing conditions.

There are method D and E that give procedures to determine some factors.

ISO 6336:2006 and ISO 6336:2019 use only method A and B.

The factors are usually defined with the subscript corresponding to the method used, for example K_{V-B} means dynamic factor according to method B

ISO 6336-2: Calculation of surface durability (pitting)

Nominal contact stress at pitch point

$$\boxed{\sigma_{H0} = Z_H \cdot Z_E \cdot Z_\epsilon \cdot Z_\beta \cdot \sqrt{\frac{F_t}{d_1 \cdot b} \cdot \frac{u+1}{u}}}$$

Zone factor

$$Z_H = \sqrt{\frac{2\cos\beta_b \cos\alpha_t'}{\cos^2\alpha_t \sin\alpha_t'}}$$

Contact ratio factor

$$Z_\epsilon = \sqrt{\frac{4-\epsilon_\alpha}{3}(1-\epsilon_\beta) + \frac{\epsilon_\beta}{\epsilon_\alpha}} \quad \text{or} \quad Z_\epsilon = \sqrt{\frac{1}{\epsilon_\alpha}}$$

Elasticity factor

$$Z_E = \sqrt{\frac{1}{\pi\left(\frac{1-\nu_1^2}{E_1} + \frac{1-\nu_2^2}{E_2}\right)}}$$

Helix angle factor

$$Z_\beta = \frac{1}{\sqrt{\cos\beta}}$$

ISO 6336-2: Calculation of surface durability (pitting)

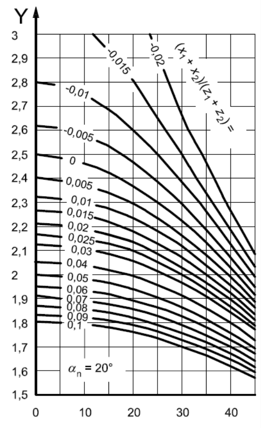

(a) Zone factor $Z_H = Y$ vs. the helix angle β

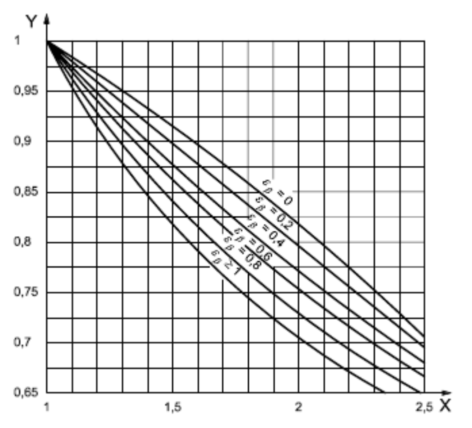

(b) Contact ratio factor $Z_\epsilon = Y$ vs. transverse contact ratio $\epsilon_\alpha = X$

Figure 23: Graphical data for $\alpha = 20°$, according to ISO 6336:2006 [14].

ISO 6336-2: Calculation of surface durability (pitting)

Contact stress

$$\boxed{\sigma_H = Z_B \cdot \sigma_{H0} \cdot \sqrt{K_A \cdot K_V \cdot K_{H\beta} \cdot K_{H\alpha}}}$$

The contact stress should be lower than the permissible contact stress:

$$\sigma_H \leq \sigma_{HP}$$

Z_B	pinion single pair tooth contact factor
K_A	application factor
K_V	dynamic factor
$K_{H\beta}$	face load factor for contact stress
$K_{H\alpha}$	transverse load factor for contact stress

ISO 6336-2: Calculation of surface durability (pitting)

$$\sigma_{HP} = \frac{\sigma_{H_{lim}} \cdot Z_{NT}}{S_{H_{min}}} \cdot Z_L \cdot Z_V \cdot Z_R \cdot Z_W \cdot Z_X = \frac{\sigma_{HG}}{S_{H_{min}}}$$

σ_{HP}	permissible contact stress
$\sigma_{H_{lim}}$	allowable stress number from reference test gears (ISO 6336:5)
σ_{HG}	contact stress limit
Z_{NT}	life factor
Z_L	lubricant factor
Z_V	velocity factor
Z_R	roughness factor
Z_W	work hardening factor
Z_X	size factor
$S_{H_{min}} = 1$	minimum safety factor
S_H	safety factor

$$\boxed{S_H = \frac{\sigma_{HG}}{\sigma_H} \geq S_{H_{min}}}$$

Nominal tooth root stress

$$\sigma_{F0} = \frac{F_t}{b \cdot m_n} \cdot Y_{Fa} \cdot Y_{Sa} \cdot Y_{\epsilon} \cdot Y_{\beta}$$

To find graphical data useful to determine root bending strength, the method C presented in ISO 6336-3:1996 should be used.

Y_{Fa}	form factor
Y_{Sa}	stress correction factor
Y_{ϵ}	contact ratio factor
Y_{β}	helix angle factor

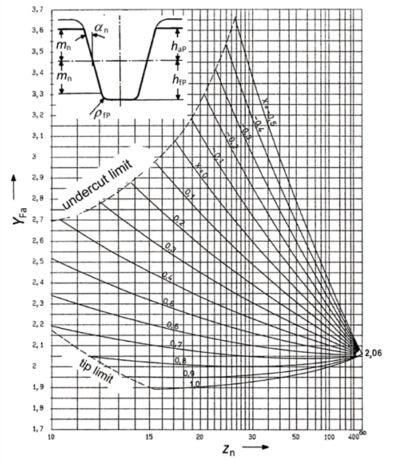

Figure 24: Form factor Y_{Fa} according to Method C for $h_{fP} = 1.25 \cdot m$, $h_{aP} = m$, $\rho_{fP} = 0.25 \cdot m$ [8].

ISO 6336-3: Calculation of tooth bending strength

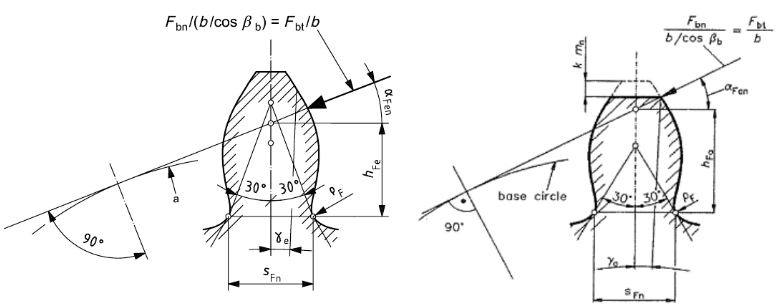

(a) Method B

(b) Method C

Figure 25: Comparison between methods B and C [8].

Method B considers that the load is applied at the first single tooth contact point.

Method C assumes that the load is applied in tooth tip.

ISO 6336-3: Calculation of tooth bending strength

Tooth root stress

$$\boxed{\sigma_F = \sigma_{F0} \cdot K_A \cdot K_V \cdot K_{F\beta} \cdot K_{F\alpha} \leq \sigma_{FP}}$$

The tooth root stress should be lower than the permissible bending stress.

K_A	application factor
K_V	dynamic factor
$K_{F\alpha}$	transverse load factor for tooth root stress
$K_{F\beta}$	face load factor for tooth root stress

ISO 6336-3: Calculation of tooth bending strength

$$\sigma_{FP} = \frac{\sigma_{F_{lim}} \cdot Y_{ST} \cdot Y_{NT}}{S_{F_{min}}} \cdot Y_{\delta relT} \cdot Y_{RrelT} \cdot Y_X = \frac{\sigma_{FG}}{S_{F_{min}}}$$

σ_{FP}	permissible bending stress
$\sigma_{F_{lim}}$	nominal stress number from reference test gears (ISO 6336:5)
σ_{FG}	tooth-root stress limit
Y_{ST}	stress correction factor
Y_{NT}	life factor for tooth-root stress
$Y_{\delta relT}$	relative notch sensitivity factor
Y_{RrelT}	relative surface factor
Y_X	size factor
$S_{F_{min}} = 1.4$	minimum safety factor
S_F	safety factor

$$\boxed{S_F = \frac{\sigma_{FG}}{\sigma_F} \geq S_{F_{min}}}$$

ISO 6336: Calculation Procedure

1. Determine the nominal stresses σ_{Ho} e σ_{Fo} – theoretical static calculation;

2. Determine the influence factors in the following order:
    - application factor K_A;
    - dynamic factor K_V considering $F_t \cdot K_A$;
    - face load factors $K_{H\beta}$ or $K_{F\beta}$ considering $F_t \cdot K_A \cdot K_V$;
    - transverse load factors $K_{H\alpha}$ or $K_{F\alpha}$ considering $F_t \cdot K_A \cdot K_V \cdot K_{H\beta}$ or $F_t \cdot K_A \cdot K_V \cdot K_{F\beta}$;

3. Determine the corrected stress σ_H e σ_F: multiply the nominal stress by the influence factors;

4. Compare a the corrected stress σ_H e σ_F with the limit stress σ_{HG} e σ_{FG} to quantify the safety factors.

Lecture 4

Summary

Efficiency of gearboxes

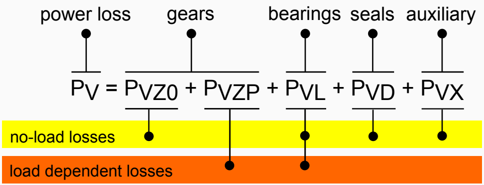

Höhn *et al.* [15]

P_{VZ0}	P_{VZP}	P_{VL}	P_{VD}
	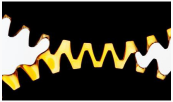		
Speed	Nominal power	Nominal power	Speed
Case geometry	Gear geometry	Bearing geometry	Seal diameter
Lubricant viscosity and density	Lubricant formulation	Lubricant formulation	Lubricant viscosity

Load dependent gear losses

$$\boxed{P_{VZP} = P_{in} \cdot H_{VL} \cdot \mu_{mZ}}$$

This equation was introduced by Ohlendorf in 1958 [16], and:

P_{in} is the input power;

H_{VL} is the gear loss factor which depends only on the gear geometry;

μ_{mZ} is the average coefficient of friction.

Let's see how this equation is determined, based on the case of a spur gear.

Load dependent gear losses

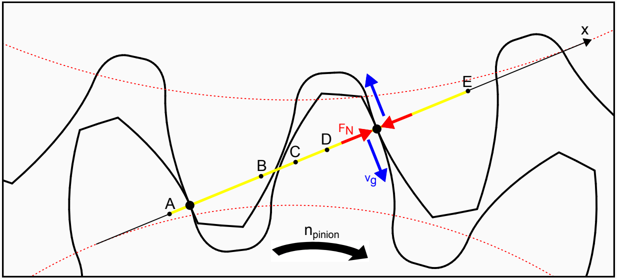

Figure 26: Sliding speed (v_g) and normal force (F_N) on the tooth contact.

At each point along the path of contact, the load-dependent gear power loss is given by the following equation:

$$P_{VZP}(x) = F_N(x) \cdot v_g(x) \cdot \mu(x)$$

μ is the local coefficient of friction.

Normal force

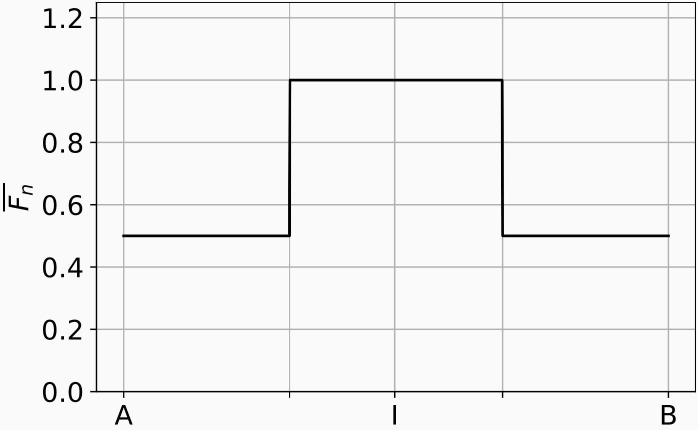

Figure 27: Load sharing function disregarding elastic effects.

Sliding speed

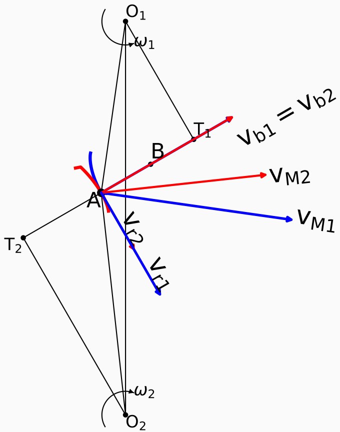

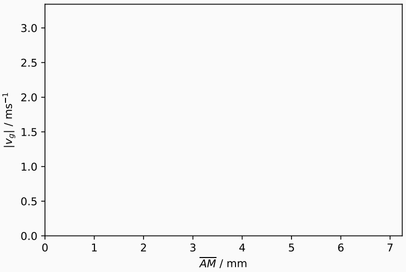

Play/Pause

Coefficient of friction

The coefficient of friction is not constant along the path of contact.

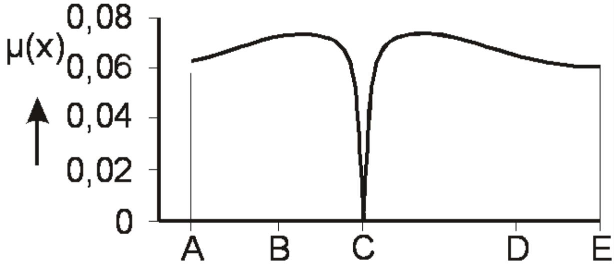

Figure 28: Coefficient of friction along the path of contact.

But given the complexity of determining an accurate coefficient of friction along the path of contact, it is commonly used an **average coefficient of friction**.

$$P_{VZP}(x) = F_N(x) \cdot v_g(x) \cdot \mu(x)$$

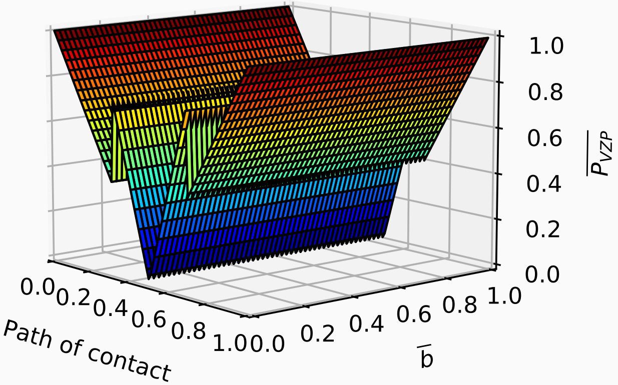

Figure 29: Normalized power loss on one tooth pair.

Gear loss factor

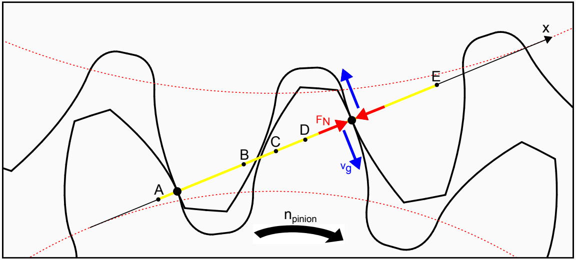

Figure 30: Sliding speed (v_g) and normal force (F_N) on the tooth contact.

$$P_{VZP}(x) = F_N(x) \cdot \mu(x) \cdot v_g(x)$$

Energy dissipated by one tooth along the path of contact:

$$E_1 = \frac{1}{\omega_1 \cdot r_{b1}} \cdot \int_A^E F_N(x) \cdot \mu(x) \cdot v_g(x) \ \mathrm{d}x$$

Gear loss factor

$$E_1 = \frac{1}{\omega_1 \cdot r_{b1}} \cdot \int_A^E F_N(x) \cdot \mu(x) \cdot v_g(x) \; \mathrm{d}x$$

The average power loss can be calculated dividing the total energy dissipated over one revolution ($z_1 \cdot E_1$) by the cycle time of one revolution ($t_1 = \frac{2 \cdot \pi}{\omega_1}$):

$$P_{VZP} = \frac{z_1 \cdot E_1}{t_1} = \frac{z_1}{t_1} \cdot \frac{1}{\omega_1 \cdot r_{b1}} \cdot \int_A^E F_N(x) \cdot \mu(x) \cdot v_g(x) \; \mathrm{d}x$$

$$P_{VZP} = \underbrace{\frac{z_1 \cdot \omega_1}{2 \cdot \pi} \cdot \frac{1}{\omega_1 \cdot r_{b1}}}_{\frac{z_1}{2 \cdot \pi \cdot r_{b1}} = \frac{1}{\pi \cdot m \cdot \cos\alpha} = \frac{1}{p_b}} \cdot \int_A^E F_N(x) \cdot \mu(x) \cdot v_g(x) \; \mathrm{d}x$$

$$P_{VZP} = \frac{1}{p_b} \cdot \int_A^E F_N(x) \cdot \mu(x) \cdot v_g(x) \; \mathrm{d}x$$

Gear loss factor

Assuming a constant coefficient of friction (average) along the path of contact:

$$P_{VZP} = \mu_{mZ} \cdot \frac{1}{p_b} \int_A^E F_N(x) \cdot v_g(x) \; \mathrm{d}x$$

Multiplying by the input power $P_{in} = F_{bt} \cdot v_{tb}$ outside the integral and dividing inside:

$$P_{VZP} = \mu_{mZ} \cdot \underbrace{F_{bt} \cdot v_{tb}}_{P_{in}} \cdot \frac{1}{p_b} \int_A^E \frac{F_N(x)}{F_{bt}} \cdot \frac{v_g(x)}{v_{tb}} \; \mathrm{d}x$$

$v_{tb} = \omega \cdot r_b$ is the tangential speed to the base circle / $\mathrm{m/s}$

$F_{bt} = \frac{M_t}{r_b}$ is the tangential force to the base radius / N

Gear loss factor

$$P_{VZP} = \mu_{mZ} \cdot \underbrace{F_{bt} \cdot v_{tb}}_{P_{in}} \cdot \underbrace{\frac{1}{p_b} \int_0^b \int_A^E \frac{f_N(x,y)}{F_{bt}} \cdot \frac{v_g(x,y)}{v_{tb}} \; \mathrm{d}x \, \mathrm{d}y}_{H_{VL}}$$

$$\boxed{P_{VZP} = \mu_{mZ} \cdot P_{in} \cdot H_{VL}}$$

To predict the power loss, H_{VL} should be calculated solving the integral (valid for spur and helical gears).

However, there are several equations to predict the gear loss factor.

Ohlendorf gear loss factor

The equation proposed by Ohlendorf is accurate mainly for spur gears:

$$\boxed{H_{VL} = \frac{\pi \cdot (u+1)}{z_1 \cdot u \cdot \cos\beta_b}\left(1 - \epsilon_\alpha + {\epsilon_1}^2 + {\epsilon_2}^2\right)}$$

$u = \frac{z_2}{z_1}$

$\epsilon_\alpha = \frac{\overline{AB}}{p_{bt}} = \frac{\sqrt{r_{a1}^2 - r_{b1}^2} + \sqrt{r_{a2}^2 - r_{b2}^2} - a' \cdot \sin\alpha'}{\pi \cdot m \cdot \cos\alpha}$

$\epsilon_1 = \frac{\overline{AI}}{p_{bt}} = \frac{\sqrt{r_{a1}^2 - r_{b1}^2} - r_1' \cdot \sin\alpha'}{\pi \cdot m \cdot \cos\alpha}$

$\epsilon_2 = \frac{\overline{IB}}{p_{bt}} = \frac{\sqrt{r_{a2}^2 - r_{b2}^2} - r_2' \cdot \sin\alpha'}{\pi \cdot m \cdot \cos\alpha}$

Coefficient of friction

$$\boxed{\mu_{mZ} = 0.048 \cdot \left(\frac{F_{bt}}{b \cdot \sum v_{r_i} \cdot R_i}\right)^{0.2} \cdot \eta^{-0.05} \cdot {R_a}^{0.25} \cdot X_L}$$

$F_{bt} = \frac{M_t}{r_b}$ is the tangential force to the base radius / N

b is the gear face width mm

$\sum v_{r_i} = v_{r_1} + v_{r_2}$ sum velocity at pitch point / $\mathrm{m/s}$

$R_i = \left(\frac{1}{r_1' \cdot \sin \alpha'} + \frac{1}{r_2' \cdot \sin \alpha'}\right)^{-1}$ relative radius at pitch point / mm

η dynamic viscosity of the lubricant at the operating temperature / $\mathrm{mPa\,s}$

R_a average roughness / $\mu\mathrm{m}$

X_L lubricant parameter

Lubricant parameter

$$\mu_{mZ} = 0.048 \cdot \left(\frac{F_{bt}}{b \cdot \sum v_{r_i} \cdot R_i} \right)^{0.2} \cdot \eta^{-0.05} \cdot {R_a}^{0.25} \cdot X_L$$

X_L lubricant parameter [17]

Mineral without additives: $X_L = 1$

Mineral with additives: $X_L = 0.85$

Synthetic with additives (PAO): $X_L = 0.65$

Lecture 5

Summary

Gear failures: introduction[1]

ISO 10825 Gears - Wear and damage to gear teeth - Terminology

- *Wear* - Desgaste
    - Normal wear
    - Abrasive wear
    - *Scoring* – gripagem a frio
    - Corrosion
    - *Fretting*
    - Overheating
    - Erosion
- *Scuffing* - Gripagem
- Permanent deformation
- Fatigue
    - *Pitting*
    - *Micropitting*
- Tooth breakage
    - Overload
    - Shear
    - Plastic deformation
    - Fatigue

[1] Lecture 5 notes by Ramiro C. Martins

Influence of lubrication and operating conditions

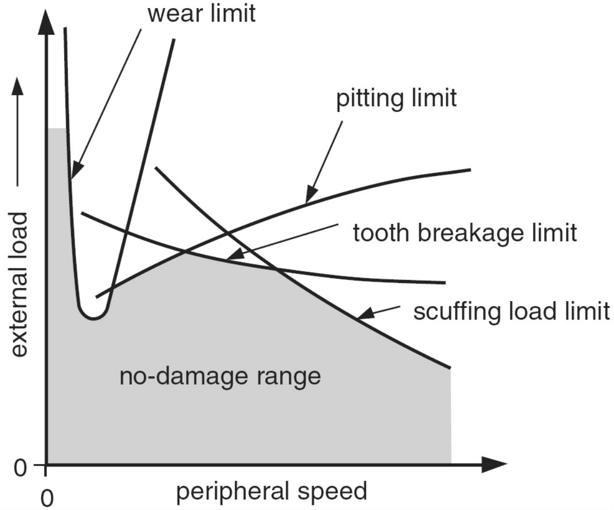

Figure 31: Peripheral speed and external load vs. failure type.

Lubrication regimes

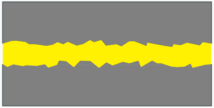

full film EHD
hidrodynamic

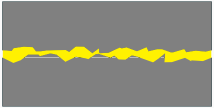

mixed film EHD

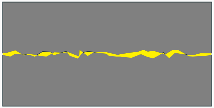

boundary EHD
solid

Figure 32: Lubrication regimes.

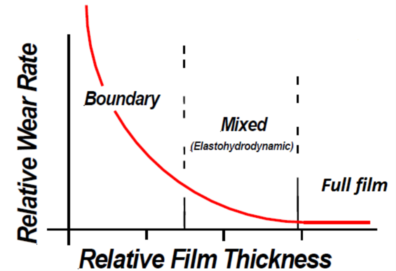

Figure 33: Relative film thickness vs. wear.

Gears operate under EHD mixed film lubrication

Normal wear (running-in wear)

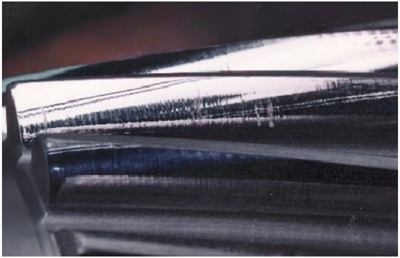

Figure 34: Gear with polished meshing surface.

Signs

Polished meshing tooth surface.

Causes

Continuous wear due to metal/metal contact under mixed/boundary film lubrication at low speed.

Solutions

This is not a problem because it is a running-in effect. Increase oil's viscosity and/or speed to decrease wear.

Moderate wear

Figure 35: Gear with moderate wear.

Signs

Surface with wear along all the flank, but larger wear above and below pitch circle.

Causes

Continuous wear due to metal/metal contact. Working under mixed film lubrication.

Solutions

Increase oil's viscosity and/or speed to decrease wear. Use lubricants with anti-wear additives.

Excessive wear

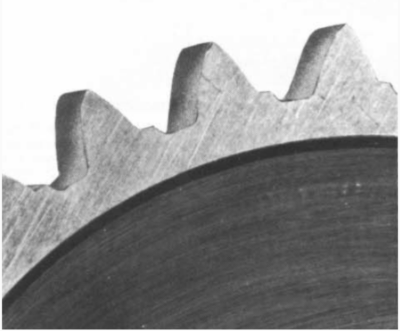

Figure 36: Gear with excessive wear.

Signs

Meshing tooth surface with large wear throughout the flank. Noise due to change in the profile form (no longer involute).

Causes

Continuous wear due to metal/metal contact under mixed/boundary film lubrication at low speed.

Solutions

Change the gear. Increase oil's viscosity and/or speed to decrease wear. Use lubricants with anti-wear additives.

Abrasive wear

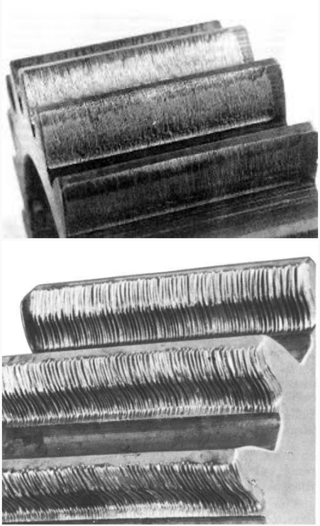

Figure 37: Gears with abrasive wear.

Signs

Tooth surface with wear marks in the radial direction. The grinding lines disappear.

Causes

Contaminants on the lubricant. Wear particles from the bearings, gears, ...

Solutions

Install an oil filter. Avoid particles in the system. Filter the oil before usage. Increase oil's viscosity.

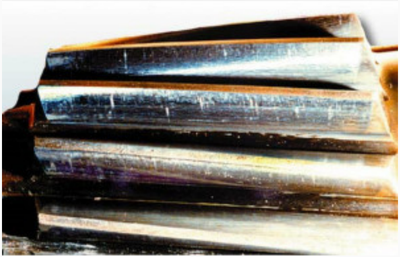

Figure 38: Gears with adhesive wear.

Signs

Tooth surface with adhesion marks in radial direction. The grinding lines disappear. Polished marks.

Causes

Lubricant film rupture due to very high contact temperature. Mixed film lubrication.

Solutions

Decrease load. Decrease lubricant temperature or increase oil flow to cool down surfaces. Increase oil viscosity. Use EP additives.

Corrosion

Figure 39: Gears with corrosion.

Signs

Surfaces with red/brown areas (depends on the chemical agent).

Causes

Contamination with acid, water, etc. Sometimes the EP additives are quite reactive.

Solutions

Avoid the corrosive medium. Use seals. Change lubricant and flush the gearbox.

Fretting corrosion

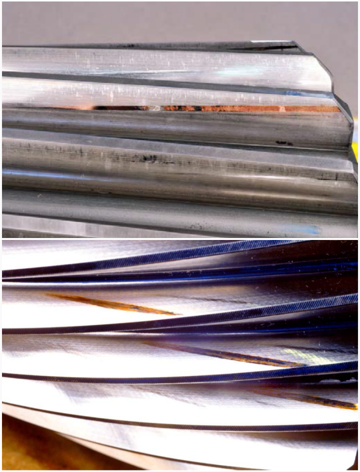

Figure 40: Gears with fretting corrosion.

Signs

Longitudinal marks on the flank with red/brown coloring. Flank degradation.

Causes

Repeated small movements of one contacting surface over another. Stationary gears may be affected if subjected to structure-borne vibrations (during transport).

Solutions

Avoid vibrations while stopped or keep them rotating.

Overheating

Figure 41: Gears with failure due to overheating .

Signs

Deformed tooth and oxidized (black). Temper colors are present and frequently scuffed areas and plastic deformation are also found.

Causes

Inadequate lubrication or insufficient backlash. Temperature above the temper point.

Solutions

Improve lubrication. Improve cooling. Increase oil flow.

Scoring

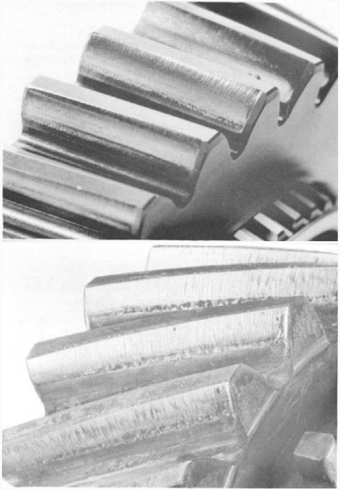

Figure 42: Gears with scoring – gripagem a frio.

Signs

Tooth surface with adhesion marks in radial direction. Polished marks with ice aspect. Evolves with time.

Causes

Film rupture due to very high load and low speed. Occurs with the lubricant operating at the normal temperature.

Solutions

Increase specific film thickness (increase viscosity or speed). Use EP additives.

Scuffing

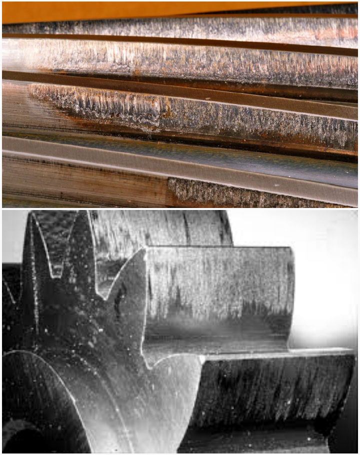

Figure 43: Gears with scuffing (gripagem).

Signs

Noise and vibration. Banded roughness in the direction of sliding (mild to severe scuffing).

Causes

Disrupted lubricant film causes local welding of the tooth flanks (transfer of material). Boundary lubrication and high $P \cdot V$.

Solutions

Decrease the contact temperature and/or load. Change gear geometry. Increase viscosity and use EP additives.

Permanent deformation

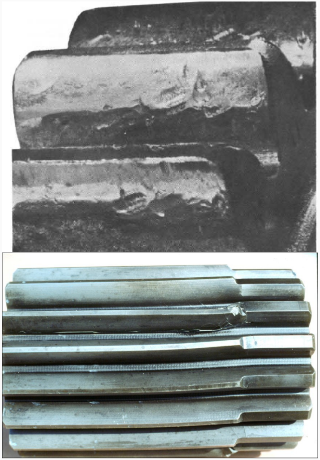

Figure 44: Gears with permanent deformation.

Signs

Noise and vibration. Depressions in tooth flanks.

Causes

Overload. Low yield strength of the material. Passage through mesh of foreign bodies.

Solutions

Change gear. Decrease load. Change gear material.

Pitting

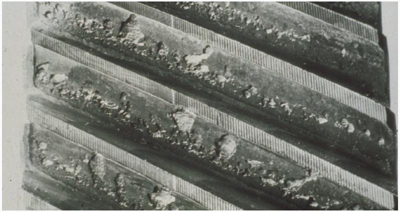

Figure 45: Gears with pitting.

Signs

Noise and vibration. Flank with scattered holes. Holes with lines typical of crack propagation.

Causes

High contact pressure. Low fatigue limit strength of the material.

Solutions

Decrease contact pressure. Increase fatigue limit strength of the material.

Figure 46: Gears with spalling.

Signs

Noise and vibration. Flank with holes. Holes with borders perpendicular to the surface. Crack in the transition of the hardened layer.

Causes

High contact pressure. Low fatigue limit strength of the material. Case hardened layer thickness is insufficient.

Solutions

Increase the hardened depth. Decrease contact pressure. Increase fatigue limit strength of the material. Increase material hardness.

Micropitting

Figure 47: Gears with micropitting.

Signs

Flank with grayish aspect (tooth deddendum). Continuous wear on the affected zone.

Causes

Insufficient specific film thickness. Lubricant promotes low protection to micropitting. Cracks initiates on the surface whith micropitts smaller than 20 μm of depth.

Solutions

Increase specific film thickness. Use a better lubricant (aditives).

Tooth breakage due to overload

Figure 48: Gears with tooth breakage due to overload.

Signs

Several tooth broken. Brittle fracture, ductile fracture or semi-brittle fracture.

Causes

Very high load. Low material toughness. Low yield strength.

Solution

Decrease load. Increase material toughness. Increase yield strength of the material.

Tooth shear

Figure 49: Gears with tooth shear.

Signs

The appearance of the sheared surfaces is similar to that of machined surfaces.

Causes

Low-strength material which are meshed with gears made of stronger materials. Bearing failure causing increase in axis distance promoting shocks.

Solutions

Avoid overload. Improve gear material properties.

Tooth breakage due to fatigue

Figure 50: Gears with tooth breakage due to fatigue.

Signs

Noise and vibration. Tooth breakage.

Causes

High tooth root stress. Low fatigue limit strength of the material. Material defects. Misalignment causes overload.

Tooth breakage due to fatigue

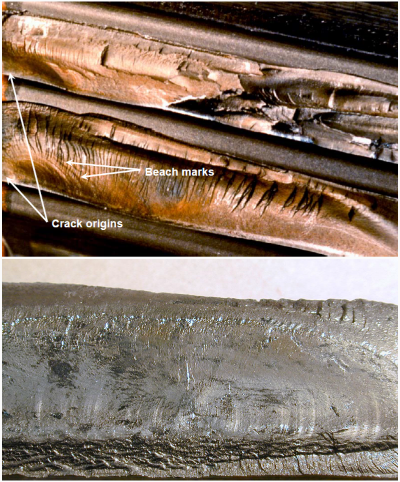

Figure 51: Gears with tooth breakage due to fatigue.

Solutions

Decrease tooth root stress. Increase fatigue limit strength of the material. Correct misalignment.

Problems

Summary

Assignments

Assignments A5 and A6

Available on the Course Contents:

“Assignments” proposed for Complements of Machine Elements

Efficiency of a spur gear

Consider a spur gear with $z_1 = 25$, $z_2 = 40$, $m = 2\,\mathrm{mm}$, $\alpha = 20^\circ$ and $b = 20\,\mathrm{mm}$ with a surface finishing that assures $R_a = 0.6\,\mu\mathrm{m}$. The torque transmitted is $T_1 = 130\,\mathrm{N\,m}$ at $n = 1500\,\mathrm{rpm}$. The gear is to be lubricated with a PAO ISO VG 150 operating at $65\,^\circ\mathrm{C}$.

Determine:

1. Gear loss factor (Ohlendorf) for the gear without profile shift;
2. Determine the profile shift to equalize the specific sliding;
3. Gear loss factor (Ohlendorf) with the profile shift;
4. Coefficient of friction (Schlenk);
5. Gear power loss and efficiency.

References

[1] Juvinall, Robert C. and Kurt M. Marshek: *FUNDAMENTALS OF MACHINE COMPONENT DESIGN*. **Wiley, 2017.**

[2] Budynas, Richard G.: *Shigley's mechanical engineering design*. **McGraw-Hill, 2014, ISBN 9789339221638.**

[3] Castro, Paulo M. S. Tavares de and Sérgio M. O. Tavares: *Capacidade de carga das rodas dentadas*, 2013.

[4] Wallace, E.L.: *Machine Design: A Manual of Practical Instruction in Designing Machinery for Specific Purposes, Including Specifications for Belts, Screws, Pins, Gears, Etc., and Many Working Hints as to Operation and Care of Machines*. **American technical society, 1918.**

[5] Black, P.H., P.H. Black, and O.E. Adams: *Machine Design*. **McGraw-Hill, 1955, ISBN 9780070850378.**

[6] Verein Deutscher Ingenieure: *VDI2736 - Part 2*. **Number June. 2014.**

[7] Haberhauer, Horst: *Maschinenelemente*. **Springer Berlin Heidelberg, Berlin, Heidelberg, 2018, ISBN 978-3-662-53047-4.**

[8] ISO 6336-3:1996: *Calculation of load capacity of spur and helical gears. Part 3: Calculation of tooth bending strength*. **1996.**

[9] Henriot, Georges: *Engrenages parallèles - Étude géométrique*.

[10] Henriot, G.: *Traité théorique et pratique des engrenages*. **Dunod, 1961, ISBN 2.04.005836.2.**

[11] Vullo, Vincenzo: *Gears*, volume 10 of *Springer Series in Solid and Structural Mechanics*.
Springer International Publishing, Cham, 2020, ISBN 978-3-030-38631-3.

[12] ISO 6336-1:2006: *Calculation of load capacity of spur and helical gears*.
2006:13, 2006.

[13] ISO 6336-1:2019: *Calculation of load capacity of spur and helical gears - Part 1: Basic principles, introduction and general influence factors*.
2019.

References iv

[14] ISO 6336-2:2006: *Calculation of load capacity of spur and helical gears. Part 2: Calculation of surface durability (pitting).* **2006.**

[15] Höhn, B. R. R, Klaus Michaelis, and T Völlmer: *Thermal Rating of Gear Drives Balance Between Power Loss and Heat Dissipation.* **AGMA Technical Paper, 96:12, 1996.**

[16] Ohlendorf, H: *Verlustleistung und Erwärmung von Stirnrädern.* **PhD thesis, Dissertation TU München, 1958.**

[17] Fernandes, Carlos M.C.G., Pedro M.T. T Marques, Ramiro C. Martins, and Jorge H.O. Seabra: *Gearbox power loss. Part II: Friction losses in gears.* **Tribology International, 88:309–316, aug 2015, ISSN 0301679X.**